Inelastic breakup in heavy-ion reactions

A. Bonaccorso
Istituto Nazionale di Fisica Nucleare, 56100 Pisa, Italy

D. M. Brink
Department of Theoretical Physics, 1 Keble Road, Oxford OX1 3NP, United Kingdom
(Received 21 February 1992)

In this paper we discuss inelastic breakup, which is one of the direct components of the inclusive energy spectra for transfer to the continuum reactions. There is inelastic breakup when a nucleon is emitted by the projectile without being absorbed by the target but at the same time the target undergoes an inelastic excitation because of the final-state interaction. We estimate the inelastic breakup from the imaginary part of the nucleon-nucleus optical potential. The basic assumption is that inelastic processes give the major contribution to the surface part of the absorptive potential. Our approach allows inelastic breakup to be distinguished from elastic breakup in which the target remains in its ground state and from other types of absorptive effects like transfer to single particle and/or compound nucleus resonances and we discuss the energy evolution of the various processes.

PACS number(s): 25.70.−z

I. INTRODUCTION

This paper is concerned with heavy-ion reactions in which a single nucleon is removed from the projectile and transferred to a continuum state of the target nucleus. An example is ^{208}Pb(^{20}Ne,^{19}Ne)^{209}Pb*, where the neutron from ^{20}Ne is transferred into an unbound state in ^{209}Pb. An approximate formula given in the appendix of Ref. [1] expressed the probability of transfer to the continuum in terms of the scattering matrix S_{00} for elastic scattering of the transferred neutron by the target. The S matrix is unitary, hence S_{00} includes the effects of elastic scattering, inelastic scattering, and transfer to resonance states. If the interaction of the neutron with the target is represented by an optical model, then the effects of both transfer of the neutron into resonance states of the target and inelastic scattering are included in the imaginary part of the optical potential.

In order to understand experimental spectra it is necessary to disentangle the two processes which give rise to the absorption. An inclusive experiment measures the total transfer cross section which has components due to elastic breakup, inelastic breakup, and resonance absorption. The behavior of the spectra depends on how much each process contributes and this in turn depends on the incident energy. At low incident energy and for final ejectile energies higher than the beam energy the spectra have some bumps [2–5]. These have been shown [3,4,6] to be due to transfer to high angular momentum states of the target. In this case the calculations in [3] show that the elastic breakup is very small. A part of the absorption is due to inelastic breakup and it is important to have an estimate of this contribution. The remaining part gives the strength of the transfer to single particle resonances [6]. On the other hand, an experiment in which the light particle emitted by the projectile is detected at forward angles in coincidence with the projectilelike fragment gives the direct component of the reaction. This is the sum of the elastic and inelastic breakup contributions.

Therefore one is interested in estimating the strength of the inelastic breakup. The spectrum obtained by adding this to the elastic breakup part discussed in Ref. [2] can be compared with the results of a coincidence experiment. The difference between the absorption as discussed in Refs. [1] and [2] and the inelastic breakup gives information on the single particle strength.

In Ref. [2] the final-state interaction of the neutron with the target was represented by an optical potential. The transfer to the continuum had a breakup part and an absorptive part. The absorption included contributions from compound nucleus formation and inelastic breakup. It was also shown that the scattering of the neutron by the target could be calculated by perturbation theory (Born approximation) if the energy of the incident heavy ion was large enough. The Born approximation formulas obtained in Ref. [2] were

$$\frac{dP_{\text{breakup}}}{d\varepsilon_f} = \frac{m}{\hbar^2 k_f}\frac{1}{2\pi v^2\hbar^2} \times \int d\mathbf{b}\,|\tilde{V}_2(\mathbf{b},k_f-k_2)\tilde{\psi}_1(\mathbf{b},k_1)|^2 , \tag{1.1}$$

$$\frac{dP_{\text{abs}}}{d\varepsilon_f} = -\frac{1}{\pi\hbar^2 v^2}\text{Im} \times \int_{-\infty}^{+\infty} d^3\mathbf{r}\,|\tilde{\psi}_1(x,y,k_1)|^2 V_2(\mathbf{r}) . \tag{1.2}$$

for the elastic breakup and absorption, respectively. V_2 is the nucleon nucleus optical potential and $\text{Im}V_2 < 0$.

A proper calculation of the inelastic breakup contribution would require a coupled-channel calculation. In this paper we obtain a simple estimate by the following argument. Neutron inelastic scattering is a surface effect and it contributes mainly to the surface region of the imagi-

nary part of the neutron optical potential. From the absorption formula (1.2) calculated in Born approximation one can see that the integrand is different from zero only in a limited region of space between the two nuclei where the surface of the target potential overlaps with the initial-state wave function. Resonance effects are neglected since they are due to the strong interaction of the neutron with the interior of the potential. The results given in Fig. 6 of Ref. [2] show that the perturbation formula (1.2) misses the resonance effects but is accurate at high neutron final energies where the imaginary part of the neutron-nucleus optical potential is almost certainly due to inelastic scattering. Hence using Eq. (1.2) to calculate the absorption corresponds to considering that part of the optical potential that describes direct inelastic excitation of the target.

In Sec. II we generalize Eq. (1.1) to obtain the inelastic breakup component of transfer to the continuum. This involves summing contributions to all excited states of the target. In Sec. III we show that this sum can be replaced by the imaginary part of a phenomenological optical potential. We find that the inelastic breakup formula corresponds to Eq. (1.2), which gives the absorption calculated in Born approximation. Section IV contains the discussion of some numerically calculated spectra and finally we give some conclusions in Sec. V.

II. INELASTIC BREAKUP

The elastic breakup formula Eq. (1.1), which is based on the approximate propagator $G \approx G_0 V_2 G_1$ discussed in Ref. [2], can be generalized to include cases in which the neutron scatters inelastically from the target. The neutron bound to a projectile (represented by a potential V_1) is excited into the continuum when it strikes the target (represented by the potential V_2). But now the target can also be excited from some initial state α to some final state β. The potential V_1 is assumed to move along a classical path with constant velocity $\mathbf{v}$[1] and V_2 is fixed. That is, we work in a frame of reference where the target is at rest. The neutron-target total wave function in the initial and final channels is

$$\Phi_i = \phi_i \chi_\alpha \ , \quad \Phi_f = \phi_f \chi_\beta \ . \tag{2.1}$$

Here χ_α is the ground state of the target with energy $\varepsilon_\alpha = 0$ and χ_β is an excited state. Initially the neutron is bound to the moving potential $V_1(\mathbf{r}-\mathbf{v}t)$. The initial neutron wave function is

$$\phi_i(\mathbf{r},t) = \psi_i(\mathbf{r}-\mathbf{v}t)\exp(i/\hbar)[m\mathbf{v}\cdot\mathbf{r} - (\tfrac{1}{2}mv^2+\varepsilon_i)t)] \ . \tag{2.2}$$

The interaction with the potential V_2 causes the neutron to make a transition to a continuum final state whose wave function is

$$\phi_f(\mathbf{r},t) = \exp(i\mathbf{k}\cdot\mathbf{r} - \varepsilon_f t/\hbar) \ . \tag{2.3}$$

It consists of a plane wave representing the final state of the neutron and a time-dependent part containing the final energy

$$\varepsilon_f = \varepsilon_\beta + \hbar^2 k^2/2m \ , \tag{2.4}$$

which is the sum of the excitation energy ε_β of the final nuclear state and the kinetic energy of the neutron. At the same time the target is excited to an internal state χ_β with excitation energy ε_β.

The transition amplitude calculated by time-dependent perturbation theory is

$$A_{\beta\alpha}(\mathbf{k}) = \frac{1}{i\hbar}\int dt \int d\mathbf{r}\, \phi_f^*(\mathbf{r},t) V_{\beta\alpha}(\mathbf{r}) \phi_i(\mathbf{r},t) \ , \tag{2.5}$$

where we have already integrated over the target internal coordinates. Here $V_{\beta\alpha}(r)$ is the matrix element of the neutron-nucleus interaction between the states β and α. In the following we choose the z axis parallel to the direction of relative motion. The time integral in Eq. (2.5) can be calculated by making a change of variables from t to $z' = z - vt$. As in Ref. [2] the result is expressed in terms of the Fourier transforms of $V_{\beta\alpha}$ and ψ_i with respect to the z axis as

$$A_{\beta\alpha}(\mathbf{k}) = \frac{i}{v\hbar}\int d\mathbf{b} \exp(-i\mathbf{k}_\perp\cdot\mathbf{b}) \tilde{V}_{\beta\alpha}(\mathbf{b}, k_z - k_2) \times \tilde{\psi}_i(\mathbf{b}, k_1) \ , \tag{2.6}$$

where $\mathbf{b}$ is the projection of the vector $\mathbf{r}$ on the (x,y) plane, k_z is the z component of $\mathbf{k}$, $\mathbf{k}_\perp$ is the component of $\mathbf{k}$ parallel to the (x,y) plane, and

$$\begin{aligned} k_1 &= (\varepsilon_f - \varepsilon_i + \varepsilon_\beta - \tfrac{1}{2}mv^2)/\hbar v \ , \\ k_2 &= (\varepsilon_f - \varepsilon_i + \varepsilon_\beta + \tfrac{1}{2}mv^2)/\hbar v \ . \end{aligned} \tag{2.7}$$

The reaction Q value is $Q = -(\varepsilon_f - \varepsilon_i + \varepsilon_\beta) < 0$.

It is interesting to note the similarity between Eq. (2.6) and Eq. (A10) of the Appendix which gives the eikonal form of the amplitude for scattering of a free neutron when the target makes a transition from channel α to channel β. Considering that in Eq. (A10) $k_\beta = k_z$ and k_α is the momentum in the incident channel corresponding to k_2 in Eq. (2.6) we notice that the characteristic of Eq. (2.6) is to depend on the neutron initial momentum distribution $\tilde{\psi}_i(\mathbf{b}, k_1)$ which is determined by its wave function in the projectile.

The total transfer probability to a final state with the target nucleus excited to a state β and a neutron with momentum in an interval $dk_\perp^2 dk_z$ is

$$dP = \frac{1}{8\pi^3}\sum_{\beta\neq\alpha}\int d^2k_\perp dk_z |A_{\beta\alpha}(\mathbf{k})|^2 \ . \tag{2.8}$$

If we make the approximation that

$$\varepsilon_f - \varepsilon_\beta = \hbar^2(k_\perp^2 + k_z^2)/2m \approx \hbar^2 k_z^2/2m \ , \tag{2.9}$$

that is put $k_z = k_\beta$ where $\hbar^2 k_\beta^2/2m = \varepsilon_f - \varepsilon_\beta$, then arguments analogous to those used in Ref. [2] give an energy spectrum

$$\frac{dP_{\text{cont}}}{d\varepsilon_f} = \frac{1}{v\hbar}\frac{1}{2\pi v^2\hbar^2} \times \sum_{\beta\neq\alpha}\int d\mathbf{b} |\tilde{V}_{\beta\alpha}(\mathbf{b}, k_\beta - k_2)\tilde{\psi}_i(\mathbf{b}, k_1)|^2 \ . \tag{2.10}$$

Here we approximated k_β in the denominator by $mv/\hbar$, that is, we neglect the dependence on ε_f. Some off-shell effects are neglected when we make these approximations.

III. INELASTIC SCATTERING AND THE OPTICAL POTENTIAL.

In this section we make a connection between Eqs. (2.10) and (1.2). This can be done in a direct way if the scattering of the neutron by the target is calculated in the eikonal approximation.

The transition amplitude for elastic scattering of a neutron by an effective potential given by the eikonal approximation is [8]

$$f_E=\frac{k}{2\pi i}\int_0^\infty d^2\mathbf{b}\, e^{-i\mathbf{k}_\perp\cdot\mathbf{b}}[e^{i\chi(k,\mathbf{b})}-1]\ , \tag{3.1}$$

where $\chi(k,\mathbf{b})$ is proportional to the phase shift and in terms of the optical potential is given by

$$\begin{aligned}\chi_{\rm opt}(k,\mathbf{b})&=-\frac{1}{\hbar v}\int_{-\infty}^{+\infty}V_{\rm opt}(\mathbf{b},z)dz\\&=-\frac{1}{\hbar v}\int {\rm Re}V_{\rm opt}dz-\frac{i}{\hbar v}\int {\rm Im}V_{\rm opt}dz\ .\end{aligned} \tag{3.2}$$

On the other hand, in the Appendix we have shown that the eikonal approximation can be used to get the elastic scattering amplitude in a coupled-channel calculation and we obtained

$$f_\alpha=\frac{k}{2\pi i}\int_0^\infty d^2\mathbf{b}\, e^{-i\mathbf{k}_\alpha\cdot\mathbf{b}}[g_\alpha(\mathbf{b},z=\infty)-1]\ , \tag{3.3}$$

where g_α is the elastic channel wave function amplitude calculated by the eikonal approximation and given by Eq. (A16) as

$$g_\alpha(\infty)\sim\exp\left[-\frac{1}{2\hbar^2v^2}\sum_{\beta\neq\alpha}|\tilde V_{\beta\alpha}(\mathbf{b},k_\beta-k_\alpha)|^2\right]\ . \tag{3.4}$$

Therefore inserting Eq. (3.2) into (3.1) and Eq. (3.4) into (3.3) and then comparing (3.3) with (3.1) we get

$$\int_{-\infty}^{+\infty}{\rm Im}V_{\rm opt}(\mathbf{b},z)dz=-\frac{1}{2\hbar v}\sum_{\beta\neq\alpha}|\tilde V_{\beta\alpha}(\mathbf{b},k_\beta-k_\alpha)|^2\ . \tag{3.5}$$

Equation (3.5) is interesting because it relates the phenomenological optical potential to the coupled-channel matrix elements. A similar result was obtained by Bonaccorso and Brink in 1982 starting from Feshbach's formalism [cf. Eq. (20) of Ref. [7]].

In the coupled-channel calculation k_α is the neutron momentum in the incident channel. In our transfer model k_2 defined in Eq. (2.6) is the neutron momentum relative to the target. Then using Eq. (3.5) with $k_\alpha=k_2$ in Eq. (2.10) we get that the inelastic breakup probability formula is equivalent to Eq. (1.2) which gives the absorption calculated in Born approximation.

IV. ENERGY SPECTRA

We have shown that the inclusive cross section for transfer to the continuum is made up of several components. Their relative strength depends on the projectile target combination and on the incident energy. In this section we illustrate this by showing results for different energies and projectile target combinations. The spectra are calculated with the formulas given in the previous section and in Ref. [3]. The effect of spin in resonant transfer was taken into account according to the method in the Appendix of Ref. [3]. The numerical parameters used in the calculations are the same as in Ref. [3]. We have chosen cases for which experimental data exist.

One problem related to the understanding of experimental data consists in the so-called "extraction of the background." The background is known to be due to direct types of reactions like breakup in which the emitted nucleon does not interact much with the target. Some experimental spectra like the ones of Refs. [4,5] show bumps which seem to be superimposed on a very wide background. As we mentioned in the Introduction it has been shown that these bumps are due to transfer to single particle resonance states in the target [3,4,6]. It is therefore useful to have an estimate of the background to understand the relative strength of the transfer to resonance states compared to the breakup. This relative strength depends on the states which are available in the initial and final nucleus. If the states are such that there are good matching conditions, then transfer will be favored with respect to breakup.

Figures 1–3 show calculations corresponding to the experimental data of Refs. [4,5]. Figures 4 and 5 are related to some data of Ref. [10]. In Ref. [10] an estimate of the transfer and direct component of the spectra was attempted.

Figures 1 and 2 show the reaction

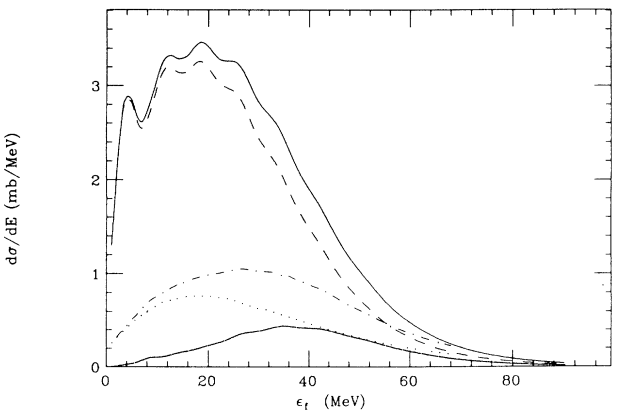

FIG. 1. Spectrum of the reaction ^{208}Pb(^{20}Ne,^{19}Ne)^{209}Pb at $E_{\rm inc}=40$ MeV/nucleon. Numerical parameters are as in Ref. [3], cf. Ref. [4] for a similar experimental spectrum. The full curve gives the total cross section for transfer to the continuum, the dot curve gives the inelastic breakup while the close-dotted curve gives the elastic breakup, the dot-dashed curve gives the total breakup, and the dashed curve gives the total absorption calculated with the optical model.

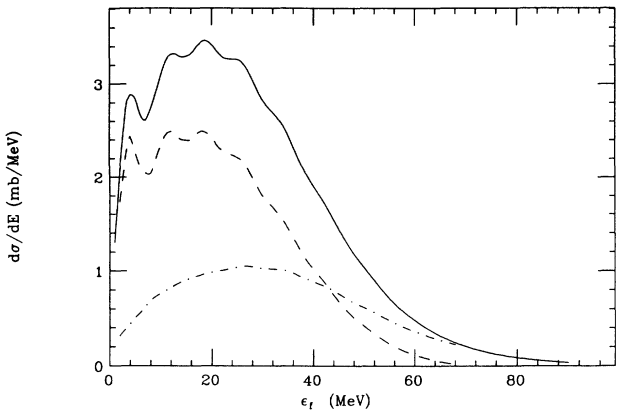

FIG. 2. Same reaction and energy as Fig. 1. The dashed curve gives the resonant transfer, the dot-dashed curve gives the sum of the elastic and inelastic breakup, and the solid curve gives the sum of the three processes.

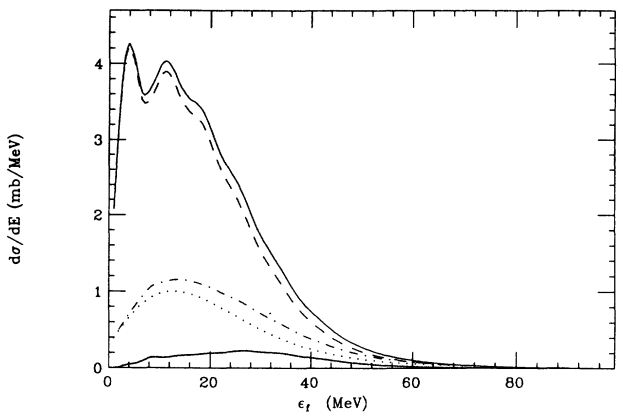

FIG. 3. Same as Fig. 1 but $E_{inc}=30$ MeV/nucleon.

^{208}Pb(^{20}Ne,^{19}Ne)^{209}Pb at $E_{inc}=40$ MeV/nucleon. The full curve in Fig. 1 shows the total cross section for transfer to the continuum calculated according to Eqs. (2.10) and (A1) of Ref. [3] and it corresponds to the inclusive experimental cross section. The dashed curve in Fig. 1 represents the total absorption spectrum, while the close-dotted curve shows the elastic breakup both calculated as in Ref. [3] using the optical model to describe the scattering of the neutron on the target. The full curve is the sum of the dashed and close-dotted curves. The dotted curve represents the inelastic breakup calculated using Eq. (1.2). This is justified by the arguments developed in Sec. I and II of this paper. The cross sections are calculated from the transfer probability with Eq. (2.10) of Ref. [3]. Finally the dot-dashed curve gives the sum of the elastic and inelastic breakup. This is the spectrum that should be seen in a coincidence experiment between the projectilelike fragment and the light particles emitted in forward direction and it gives a contribution to the background mentioned earlier.

Figure 2 shows the same reaction at the same energy as before. The dot-dashed curve is again for the elastic plus inelastic breakup while the dashed curve gives the transfer cross section which has been obtained by subtracting this from the total cross section represented by the full curve. One notices that in this case the elastic plus inelastic breakup accounts for about one-third of the cross section while the resonant transfer is quite strong and accounts for two-thirds of the cross section at the peak. On the tail the spectrum is just given by the elastic plus inelastic breakup. This is due to the fact that at very high final neutron energies there are no single particle or compound nucleus resonance states available in the target.

Figure 3 shows the same reaction at $E_{inc}=30$ MeV/nucleon. It shows that the elastic plus inelastic breakup is smaller than before and it accounts for about a quarter of the cross section at the peak. Also it is mainly given by inelastic breakup (dotted curve) while the elastic breakup contribution is very small (close-dotted curve). At low energy we see then that resonant transfer dominates the cross section because the optimum Q-value matching condition discussed at the end of Ref. [3] favors final energies of the neutron which correspond to available resonance single particle states in the target.

Figures 4 and 5 show the reaction ^{208}Pb(^{14}N,^{13}N)^{209}Pb at $E_{inc}=60$ MeV/nucleon. The incident energy is higher in this reaction and also the projectile is different. In Ref. [3] we showed that the shape of the total spectrum was related to the neutron momentum distribution in the initial nucleus. Figure 4 shows that at such high energies the elastic breakup (close-dotted curve) has taken over from the inelastic breakup (dotted curve). The total absorption has also been reduced with respect to the previous figures. The next figure shows the same reaction at the same energy as Fig. 4. The dashed curve gives the resonant transfer, and the dot-dashed curve is for the elastic plus inelastic breakup. One notices that the direct component of the spectrum is larger than the transfer component at this energy.

There are several remarks to be done about the background. At low incident energy (Fig. 3) it is mainly due

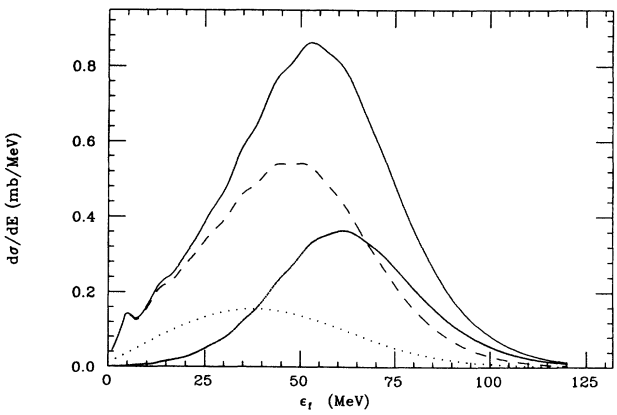

FIG. 4. Spectrum of the reaction ^{208}Pb(^{14}Ni,^{13}Ni)^{209}Pb at $E_{inc}=60$ MeV/nucleon. Numerical parameters are as in Ref. [3]. The corresponding proton transfer experimental spectrum was given in Ref. [10]. Same notation as Fig. 1.

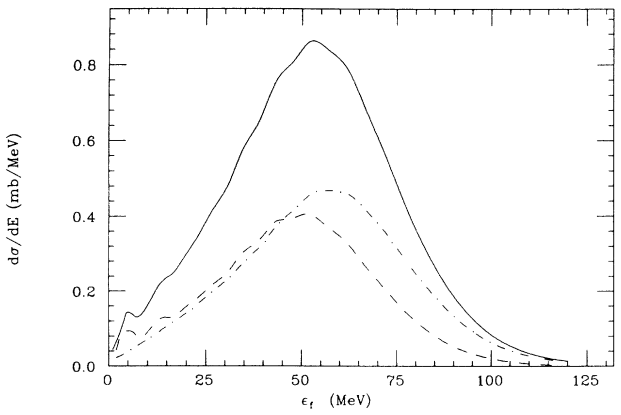

FIG. 5. Same reaction and energy as Fig. 4. Notation as in Fig. 2.

to inelastic breakup. Also we notice that the maxima of the elastic and inelastic spectra are well separated. The elastic breakup is centered around the incident energy per nucleon while the inelastic breakup is centered around $\varepsilon_f=\frac{1}{2}mv^2-|\varepsilon_i|$ according to the discussion in Ref. [3]. As the incident energy increases (Figs. 1 and 2), the elastic breakup becomes dominant and at very high energy the background due to elastic and inelastic breakup has a magnitude larger than the compound nucleus component. This is clear in Fig. 5 where the dot-dashed curve gives the background while the dashed curve gives the transfer component which in this case is due to compound nucleus resonances [3]. The strong increase of the elastic breakup as the incident energy increases can be understood by looking at Eq. (1.1). In Ref. [3] we showed that for a Woods-Saxon potential an approximate form of its Fourier transform which appears in Eq. (1.1) is given by

$$\tilde{V}_2(\mathbf{b},k_f-k_2)=(2\pi ba)^{1/2}V_2(b)e^{-(k_f-k_2)^2ab/2}, \qquad (4.1)$$

where a is the diffuseness parameter. Equation (4.1) has a maximum when $|k_f-k_2|$ is a minimum and this corresponds to $\varepsilon_f\approx\frac{1}{2}mv^2$. Also the maximum value of the exponential term in (4.1) is given by $\exp[-(\varepsilon_i/\hbar v)^2ab/2]$. This shows how the elastic breakup increases as the incident energy increases because of the $1/v^2$ dependence in the exponential where v is the incident velocity. It also shows that the elastic breakup is expected to be larger for small separation energies ε_i of the neutron in the initial nucleus.

This has interesting consequences for the α breakup. It is known [11] that in fragmentation reactions often the most populated final channel is the α channel and this happens when the separation energy for an α particle from the projectile is smaller than for a neutron or a proton.

On the other hand, the energy dependence of the absorption in Eq. (1.2) is contained only in the initial-state momentum distribution $\tilde{\psi}_1(\mathbf{b},k_1)$. From Eq. (2.3b) of Ref. [3] the maximum of ψ_1 corresponds to a minimum of the parameter η given by $\eta^2=k_1^2+\gamma_i^2$, where $\gamma_i^2=-2m\varepsilon_i/\hbar^2$, which gives for the maximum of $\tilde{\psi}_1$ an exponential behavior like $e^{-2\eta b}\sim e^{-2\gamma_i b}$ in which only the separation energy enters but not the incident energy. One should mention that the neutron-nucleus optical potential used in Ref. [3] and in this paper has an energy-dependent imaginary strength according to the prescription of Ref. [12] but this dependence is quite smooth and does not affect the previous discussion.

In the very low energy part of the spectrum in Fig. 5 around $\varepsilon_f=5$ MeV one may notice a little bump reminiscent of the peaks shown by the spectra in Figs. 1, 2, and 3. The peaks are due to the presence in ^{209}Pb of the three single particle resonances $k_{17/2}j_{15/2}h_{11/2}$ discussed in Ref. [3], which have a large probability of being populated by transfer because of the very favorable matching conditions.

Therefore we have shown that up to about 40 MeV/nucleon the single particle transfer effects are still dominant and the various peaks in the spectra correspond to single particle resonances populated by the transfer and were discussed in detail in Ref. [3]. The cross section for these reactions is more than two-thirds of the total inclusive cross section and by integrating over energy the contribution of every single resonance one can give an estimate of the single particle strength. This is very interesting and can be used to compare to single particle strengths obtained from transfer to bound-state reactions.

Increasing further the incident energy should give spectra in which only the direct component is important and this gives a basis for the interpretation of the so-called fragmentation which is seen at very high incident energies.

V. CONCLUSIONS

In this paper we are concerned with inelastic breakup, which is one of the direct components contributing to inclusive spectra for transfer to the continuum reactions. The eikonal approximation has been used to show that inelastic breakup corresponds to that part of the absorption that can be treated in Born approximation. In this way we are able to separate inelastic breakup from the total absorption which contains the resonant transfer.

Equation (1.2) has been calculated numerically to get some spectra which have been compared to those corresponding to the elastic breakup and total absorption and obtained by using the optical model to treat the rescattering of the transferred neutron on the target. We have shown that at low incident energies the background due to the sum of elastic and inelastic breakup is quite small while the cross section is mainly due to transfer reactions to the single particle resonance states of the target. Increasing the incident energy the elastic breakup becomes dominant and the elastic plus inelastic breakup background gives in fact the largest contribution to the cross section. Transfer is still important but to compound nucleus states rather than to single particle states. At energies higher than those studied in this paper (60 MeV/nucleon) the spectra should have the characteristics of the direct component with just one peak near the final energy corresponding to the incident energy per nucleon.

APPENDIX

In this Appendix we apply the eikonal approximation to the solution of the coupled-channel problem for neutron-nucleus scattering. The aim is to obtain the scattering amplitude in terms of the matrix elements of the coupling potential to compare with the eikonal form of the scattering amplitude given in terms of an effective optical potential. In this way we will obtain a relation between the imaginary part of the optical potential and the Fourier transform of the matrix elements of the coupling potential, Eq. (3.5) of the text.

We introduce the total neutron-nucleus scattering wave function

$$\Phi(\mathbf{r},\xi)=\sum_{\beta}\phi_{\beta}(\mathbf{r})\chi_{\beta}(\xi)\ , \tag{A1}$$

where ξ are the target internal coordinates and $\mathbf{r}$ is the position of the neutron with respect to the target. Φ satisfies the following Scrödinger equation:

$$[T+H(\xi)+V(r,\xi)-\varepsilon_f]\Phi(r,\xi)=0\ , \tag{A2}$$

where ε_f is the scattering energy. $V(r,\xi)$ is the interaction potential between the neutron and the target nucleus. The internal coordinate wave function χ_α satisfies

$$H(\xi)\chi_\alpha=\varepsilon_\alpha\chi_\alpha\ . \tag{A3}$$

Multiplying Eq. (A2) by the complex conjugate of Eq. (A1) and integrating over the internal coordinates we get the coupled-channel equation

$$-\frac{\hbar^2}{2m}\nabla^2\phi_\beta-(\varepsilon_f-\varepsilon_\beta)\phi_\beta+\sum_{\alpha}V_{\beta\alpha}\phi_\alpha=0\ , \tag{A4}$$

where $V_{\beta\alpha}=\langle\chi_\beta(\xi)|V(r,\xi)|\chi_\alpha(\xi)\rangle$ are the potential matrix elements for scattering from channel α to channel β.

In high-energy scattering the potential can be considered to vary slowly over the scale of the incident wavelength, then in the function $\phi_\beta(r)$ in Eq. (A1) we can factorize out the incident plane wave which we suppose will propagate in the z direction. Then

$$\phi_\beta=e^{ik_\beta z}g_\beta(r)\ , \tag{A5}$$

and $g_\beta(r)$ is supposed to be slowly varying. Equation (A5) leads to the eikonal approximation for the channel wave function introduced first by Glauber [9] to study nuclear scattering. Using (A5) in (A4) and neglecting the second derivative of g_β since it is supposed to be slowly varying, we obtain

$$\left[\frac{\hbar^2}{2m}k_\beta^2-\varepsilon_f+\varepsilon_\beta\right]g_\beta-i\hbar^2k_\beta\frac{\partial g_\beta}{\partial z}+\sum_{\alpha}V_{\beta\alpha}e^{-i(k_\beta-k_\alpha)z}g_\alpha=0\ . \tag{A6}$$

Equation (A6) can be simplified if we suppose that the kinetic energy in channel β is equal to the difference between the scattering energy and the target internal energy. That is,

$$\frac{\hbar^2}{2m}k_\beta^2=\varepsilon_f-\varepsilon_\beta\ , \tag{A7}$$

which is the same as Eq. (2.4) of the text. Then

$$i\hbar v_\beta\frac{\partial g_\beta}{\partial z}=\sum_{\alpha}V_{\beta\alpha}e^{-i(k_\beta-k_\alpha)z}g_\alpha\ . \tag{A8}$$

We solve the above equation with the condition that only transitions from and to the ground state $\alpha=0$ are allowed, which means that the only matrix elements different from zero are those like $V_{0\beta}$ [13]. We then get the set of equations

$$i\hbar v_0\frac{\partial g_0}{\partial z}=\sum_{\beta}V_{0\beta}g_\beta e^{-i(k_0-k_\beta)z}\ , \tag{A9}$$

$$i\hbar v_\beta\frac{\partial g_\beta}{\partial z}=V_{\beta 0}g_0e^{i(k_0-k_\beta)z}\ . \tag{A10}$$

The solution of Eq. (A10) is given by

$$g_\beta=\frac{1}{i\hbar v_\beta}\int_{-\infty}^{z}dz'V_{\beta 0}g_0e^{i(k_0-k_\beta)z'}\ . \tag{A11}$$

Substituting Eq. (A11) in Eq. (A9) gives

$$\frac{\partial g_0}{\partial z}=-\frac{1}{\hbar^2v_0v_\beta}\sum_{\beta}V_{0\beta}e^{-i(k_0-k_\beta)z}\times\int_{-\infty}^{z}dz'V_{\beta 0}g_0e^{i(k_0-k_\beta)z'}\ . \tag{A12}$$

If g_0 is supposed to be a slowly varying function of z, it can be taken outside the integral in the above equation and the solution of Eq. (A12) can be written as

$$g_0=\exp\left[-\int_{-\infty}^{\infty}\gamma(z)dz\right]\ , \tag{A13}$$

where

$$\gamma(z)=\int_{-\infty}^{z}dz'F(z-z') \tag{A14}$$

and

$$F(z-z')=-\frac{1}{\hbar^2v_0v_\beta}\sum_{\beta}V_{0\beta}(\mathbf{b},z)V_{\beta 0}(\mathbf{b},z')\times e^{-i(k_0-k_\beta)(z-z')}\ . \tag{A15}$$

Using Eq. (A15) in Eq. (A14) gives a real and imaginary part for $\gamma(z)$. The real part is symmetrical with respect to the (z,z') variables, therefore the integral in Eq. (A14) can be extended to $z=\infty$ with an extra factor of $1/2$ in front of it. We then neglect the imaginary part of $\gamma(z)$ and obtain for g_0

$$g_0=\exp\left[-\int_{-\infty}^{\infty}\gamma(z)dz\right]\approx\exp\left[-\frac{1}{2\hbar^2v^2}\sum_{\beta\neq 0}|\tilde{V}_{\beta 0}(\mathbf{b},k_\beta-k_0)|^2\right]\ . \tag{A16}$$

In Sec. III we gave the relation between the imaginary part of the nucleon-nucleus potential and the sum over excited states contained in Eq. (A16). The imaginary part of $\gamma(z)$, which is neglected, gives the so-called polarization potential which is a correction to the real optical potential.

[1] A. Bonaccorso and D. M. Brink, Phys. Rev. C **38**, 1776 (1988).
[2] A. Bonaccorso and D. M. Brink, Phys. Rev. C **43**, 299 (1991).
[3] A. Bonaccorso and D. M. Brink, Phys. Rev. C **44**, 1559 (1991).
[4] S. Fortier, S. Gales, S. M. Austin, W. Benenson, G. M. Crawley, C. Djalai, J. S. Winfield, and G. Yoo, Phys. Rev. C **41**, 2689 (1990).
[5] D. Beaumel, Y. Blumenfeld, Ph. Chomaz, N. Frascaria, J. P. Garron, J. C. Roynette, T. Suomijarvi, J. Barrette, B. Berthier, B. Fernandez, J. Gastebois, and W. Mittig, Annual Report, Orsay, 1987, p. 41.
[6] S. Gales, Ch. Stoyanov, and A. I. Vdovin, Phys. Rep. **166**, 125 (1986).
[7] A. Bonaccorso and D. M. Brink, Nucl. Phys. **A384**, 161 (1982).
[8] C. J. Joachain, *Quantum Collision Theory* (North-Holland, Amsterdam, Oxford, 1975), p. 194.
[9] R. J. Glauber, in *Lectures in Theoretical Physics*, edited by W. E. Brittin and L. G. Duhnam (Interscience, New York, 1959), Vol. 1.
[10] W. Lahmer, W. von Oertzen, A. Miczaika, H. G. Bohlen, W. Weller, R. Glasow, R. Grzonka, R. Santo, Y. Blumenfeld, N. Frascaria, J. P. Garron, J. C. Jacmart, and J. C. Roynette, Z. Phys. A **337**, 425 (1990).
[11] U. Jahnke, G. Ingold, H. Homeyer, M. Bürgel, Ch. Egelhaaf, H. Fuchs, and D. Hilscher, Phys. Rev. Lett. **50**, 1246 (1983). S. B. Gazes, H. R. Schmidt, Y. Chan, E. Chavez, R. Kamermans, and R. G. Stokstad, Phys. Rev. C **38**, 712 (1988). J. C. Steckmeyer, G. Bizard, R. Brou, P. Eudes, J. L. Laville, J. B. Natovwitz, P. P. Patry, B. Tamain, A. Thiphagne, H. Doubre, A. Péghaire, J. Péter, E. Rosato, J. C. Adloff, A. Kamili, G. Rudolf, F. Scheibling, F. Guilbaut, C. Lebrun, and F. Hanappe, Nucl. Phys. **A500**, 372 (1989); J. Pouliot, Y. Chan, D. E. DiGregorio, B. A. Harmon, R. Knop, R. G. Stokstad, C. Moisan, and R. Roy, Phys. Rev. C **43**, 735 (1991).
[12] C. Mahaux and R. Sartor, Nucl. Phys. **A493**, 157 (1989).
[13] W. N. Cottingham and D. A. Greenwood, *Introduction to Nuclear Physics* (Cambridge University, Cambridge, 1986).